

# Recent results from a Si/CdTe semiconductor Compton telescope

Takaaki Tanaka<sup>a,b</sup>, Shin Watanabe<sup>a</sup>, Shin'ichiro Takeda<sup>a,b</sup>,  
Kousuke Oonuki<sup>a,b</sup>, Takefumi Mitani<sup>a,b</sup>, Kazuhiro Nakazawa<sup>a</sup>,  
Takeshi Takashima<sup>a</sup>, Tadayuki Takahashi<sup>a,b</sup>, Hiroyasu Tajima<sup>c</sup>,  
Naoyuki Sawamoto<sup>d</sup> Yasushi Fukazawa<sup>d</sup>, Masaharu Nomachi<sup>e</sup>,

<sup>a</sup>*Institute of Space and Astronautical Science / JAXA, 3-1-1 Yoshinodai,  
Sagamihara, Kanagawa 229-8510, Japan*

<sup>b</sup>*Department of Physics, The University of Tokyo, Bunkyo, Tokyo 113-0033,  
Japan*

<sup>c</sup>*Stanford Linear Accelerator Center, Stanford, CA 94309-4349, USA*

<sup>d</sup>*Department of Physics, Hiroshima University, Higashi-Hiroshima, Hiroshima  
739-8526, Japan*

<sup>e</sup>*Department of Physics, Osaka University, Toyonaka, Osaka, 560-0043, Japan*

---

## Abstract

We are developing a Compton telescope based on high resolution Si and CdTe detectors for astrophysical observations in sub-MeV/MeV gamma-ray region. Recently, we constructed a prototype Compton telescope which consists of six layers of double-sided Si strip detectors and CdTe pixel detectors to demonstrate the basic performance of this new technology. By irradiating the detector with gamma-rays from radio isotope sources, we have succeeded in Compton reconstruction of images and spectra. The obtained angular resolution is  $3.9^\circ$  (FWHM) at 511 keV, and the energy resolution is 14 keV (FWHM) at the same energy. In addition to the conventional Compton reconstruction, i.e., drawing cones in the sky, we also demonstrated a full reconstruction by tracking Compton recoil electrons using the signals detected in successive Si layers. By irradiating  $^{137}\text{Cs}$  source, we successfully obtained an image and a spectrum of 662 keV line emission with this method. As a next step, development of larger double-sided Si strip detectors with a size of  $4\text{ cm} \times 4\text{ cm}$  is underway to improve the effective area of the Compton telescope. We are also developing a new low-noise analog ASIC to handle the increasing number of channels. Initial results from these two new technologies are presented in this paper as well.

*Key words:* gamma-ray detector, Compton telescope, Silicon strip detector, Cadmium telluride (CdTe)

## 1 Introduction

Astrophysical observations in the soft gamma-ray region ranging from about 100 keV to MeV is essential to study high energy phenomena in the universe, such as nucleosynthesis and particle acceleration. However, the observation sensitivity in this energy band is still limited due to high background, low detection efficiency, and difficulty of imaging by means of focusing technology. A Compton telescope with good energy and angular resolution is a difficult but promising way to bring a breakthrough in this energy band.

In a Compton telescope, the deposited energy and position of the gamma-ray interactions with detectors are recorded. When a gamma-ray photon is detected, its energy ( $E_{\text{in}}$ ) and the scattering angle ( $\theta$ ) can be determined as,

$$E_{\text{in}} = E_1 + E_2 \tag{1}$$

$$\cos \theta = 1 - \frac{m_e c^2}{E_2} + \frac{m_e c^2}{E_1 + E_2}, \tag{2}$$

where  $E_1$  is the energy of the recoil electron,  $E_2$  is that of the scattered gamma-ray, and  $m_e$  is the rest mass of an electron. The incident direction of a gamma-ray is determined as a cone with a vertical angle of  $\theta$ . As shown in Eq. 2, the incident direction of a gamma-ray is calculated from the observed position and deposited energy of the interactions. Therefore, position and energy resolutions of component detectors are crucial for obtaining higher angular resolution. Employing semiconductor imaging spectrometers, with their good resolutions, is hence a promising approach to realize high sensitivity Compton telescopes. From this point of view, Compton telescopes based on Si, Ge, CZT and CdTe are proposed and development is on-going by many groups [1–5].

Based on the idea proposed from our group [6,7], we are developing a new Compton telescope utilizing Si and CdTe detectors with high position and energy resolutions [8–10]. Fig. 1 shows the schematic picture of our Si/CdTe semiconductor Compton telescope. In the telescopes, Si detectors work mainly as scatterers and CdTe detectors mainly work as absorbers. This combination is efficient especially in the sub-MeV region since the probability of Compton scattering in Si is larger than that of photo-absorption in this energy band and photo-absorption is dominant in CdTe up to 300 keV. Additionally, Si works

---

*Email address:* ttanaka@astro.isas.jaxa.jp (Takaaki Tanaka).

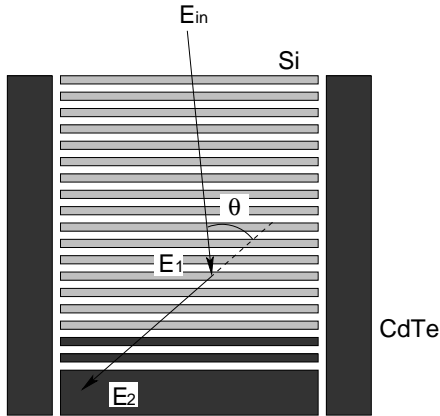


Fig. 1. Schematic picture of our Si/CdTe Compton telescope

as scatterers better than other materials with larger atomic numbers in terms of Doppler broadening, which limits the angular resolution of Compton telescopes [11]. Low noise readout system for the scatterer is also the key to realize not only good angular resolution but also lower detection threshold. The lower energy coverage is preferred to connect the band pass of Compton telescope with that of the technology using hard X-ray focusing mirror optics [12].

In this paper, we describe the recent results obtained with our prototype Si/CdTe semiconductor telescopes, which consists of six-layers of double-sided silicon strip detectors (DSSDs) and CdTe pixel detectors. We also report on the development of DSSDs with larger areas and low-noise analog ASICs with more channels for the next prototype. Basic performances and detailed discussion on the angular resolution of the prototype is reported in Watanabe et al. (2005) [10], and the vision of applications of the Si/CdTe Compton telescope to the next-generation high energy astronomy missions can be seen elsewhere [13–15].

## 2 Experimental Setup

The DSSDs used in our prototype Compton telescope have a thickness of  $300\ \mu\text{m}$ . There are 64 strips (2.56 cm long) per side and the strips on the top side are orthogonal to the ones on the back side. The strip pitch is  $400\ \mu\text{m}$  and the gap between the strips is  $100\ \mu\text{m}$ . By reading out both the p-strips and n-strips, we can obtain two-dimensional position information [16,20].

The signals from each channel of the DSSDs are read out with 32-channel low-noise analog ASIC, VA32TA, which we have developed with Ideas ASA, Norway [17,18]. The strips on the p-side are directly connected to the input pads of the ASICs, and the strips on the n-side are connected via coupling

capacitors. For the coupling capacitors and bias resistors on the n-side, we used the RC-chip, which consists of MOS capacitors and polysilicon resistors [20]. The spectral performance of the p-strips is better than that of n-strips since the strip capacitance of n-side is larger due to the more complex geometry implemented on n-side. Therefore, spectral information is obtained only from the p-strips. Fig. 2 shows a photo of the DSSD system and a spectrum of  $^{241}\text{Am}$  obtained with the DSSD operated at  $-10\text{ }^\circ\text{C}$ . The energy resolution for 59.5 keV gamma-rays is 1.3 keV (FWHM).

A photo of the CdTe pixel detector is shown in Fig. 3 (left). The detector is based on the Schottky CdTe diode device, utilizing indium as the anode and platinum as the cathode [19]. The detector has dimensions of  $18.55\text{ mm} \times 18.55\text{ mm}$  and a thickness of  $500\text{ }\mu\text{m}$ . The indium side is used as a common electrode and the platinum side is divided into 8 by 8 pixels and a guard ring with a width of 1 mm. The pixel size is  $2\text{ mm} \times 2\text{ mm}$ , and the gap between the pixels is  $50\text{ }\mu\text{m}$ . The signals from the detector are also read out with VA32TAs. A spectrum of gamma-rays from  $^{241}\text{Am}$  obtained with the CdTe pixel detector is presented in Fig. 3 (right). The detector was operated at  $-20\text{ }^\circ\text{C}$  and a bias voltage of 800 V was applied. The obtained energy resolution is 1.4 keV (FWHM) for the 59.5 keV line.

We constructed a prototype Compton telescope, utilizing the DSSDs and the CdTe pixel detectors. The arrangement of the detectors is shown in Fig. 4. The DSSDs are stacked with a gap of 5.4 mm, and two CdTe pixel detectors are placed below the DSSDs and another one is placed on the side. Analog signals from VA32TAs connected to the sensors are handled by the specially designed readout system consisting of the interface card (IFC) and the read out card (ROC) [21]. The IFC provides analog bias currents/voltages, and digital and analog signal repeater functions. The ROC performs analog-to-digital conversions, readout sequence controls, and packet generation.

In order to study an angular resolution and spectral performance of the detector, we irradiated the prototype with gamma-rays from various radio isotope sources, which were placed 350 mm above the top DSSD. The whole detector system was operated at  $-5\text{ }^\circ\text{C}$ . In the measurement, triggers from the ASICs connected to the p-strips of the DSSDs and CdTe detectors were enabled. Triggers were generated from the fast shaping amplifiers of VA32TAs with peaking time of 300 ns, and when a trigger was generated, the pulse heights of the slow shaping amplifiers of all channels latched with a delayed pulse  $2\text{ }\mu\text{s}$  after the trigger, which equals the peaking time of the slow shaping amplifiers.

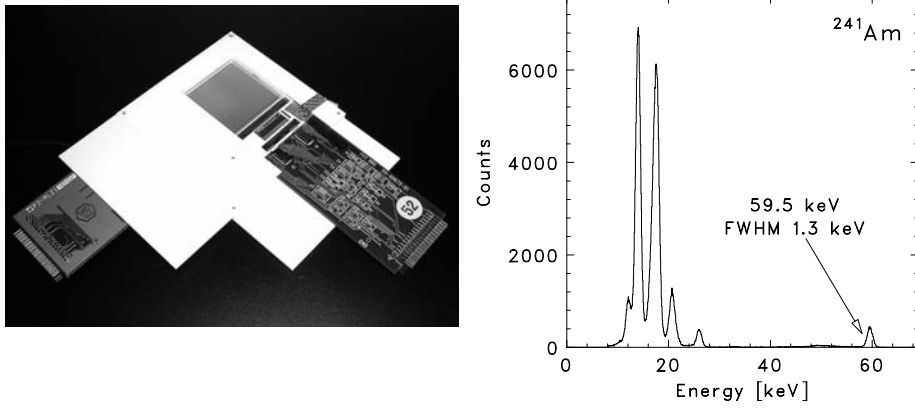


Fig. 2. The double-sided silicon strip detector (left) and a spectrum of  $^{241}\text{Am}$  obtained with it. The operation temperature is  $-10\text{ }^{\circ}\text{C}$

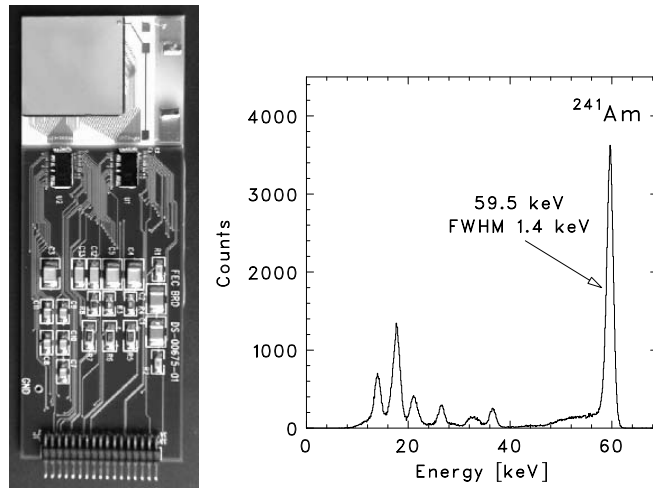


Fig. 3. Photo of the CdTe pixel detector (left) and a spectrum of  $^{241}\text{Am}$  obtained with the detector operated at  $-20\text{ }^{\circ}\text{C}$ . Applied bias voltage is 800 V.

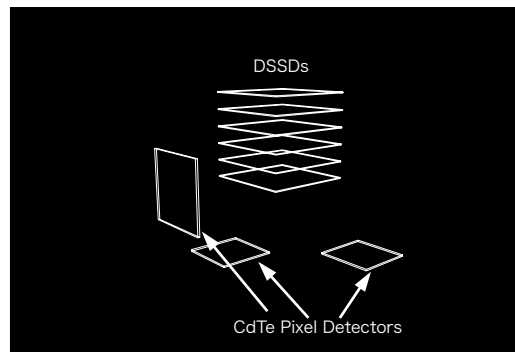


Fig. 4. Configuration of the prototype Si/CdTe semiconductor Compton telescope.

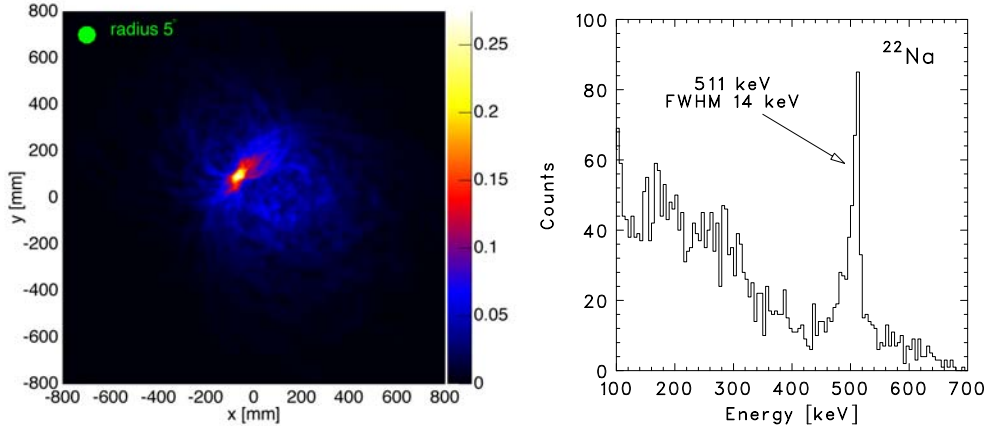


Fig. 5. A Compton-reconstructed image (left) and a spectrum of  $^{22}\text{Na}$  (right)

### 3 Data Analyses

#### 3.1 Compton Reconstruction

Compton reconstruction was performed as follows. First, “two-hit events”, one hit in a DSSD and one hit in a CdTe detector, were selected from all the events. “Hit” in a DSSD is defined such that only one strip on the p-side has a pulse height above 8 keV, and “hit” in a CdTe detector is defined such that only one pixel of the CdTe detector has a pulse height above 20 keV. Then, the scattering angle is calculated event by event, by using Eq. 2 with the observed pulse heights. Here, we assume that incident gamma-rays are scattered in the DSSD and absorbed in the CdTe pixel detector. From the calculated scattering angle and the observed hit positions, a Compton cone is drawn in the sky.

Fig. 5 (left) is a Compton reconstructed image of 511 keV gamma-rays from  $^{22}\text{Na}$ . A circle with a radius of  $5^\circ$  is shown together for comparison. The obtained resolution of the scattering angle  $\theta$  is  $3.9^\circ$  (FWHM). The obtained angular resolution is consistent with the results from Monte Carlo simulations. From our analyses of experimental data and simulation results, we confirmed the contribution of Doppler broadening is  $2.6^\circ$ , that of position resolution is  $2.7^\circ$ , and that of energy resolution is  $1.0^\circ$  (see Watanabe et al. 2005 for more details [10]).

Energy of the incident gamma-ray is calculated by summing deposited energy as shown in Eq. 1. Fig. 5 (right) shows a spectrum of gamma-rays from  $^{22}\text{Na}$ . In the spectrum, we selected the events satisfying the condition that the calculated incident angle  $\theta$  is within  $15^\circ$  from the source position. The energy resolution of the reconstructed spectrum is measured to be 14 keV (FWHM) at 511 keV.

### 3.2 Full Compton Reconstruction by Tracking Electrons

When kinetic energy of an electron is above  $\sim 250$  keV, the range of electrons in Si exceeds the thickness of one layer of the DSSD ( $300 \mu\text{m}$ ). In this case, the recoil electron deposits energy on the successive layers of the DSSDs and the direction of the electron could be tracked from the hit positions. Then, we can fully solve the Compton kinematics from the information obtained with the detectors. Although the information of the direction of electrons are smeared out by the effect of multiple scattering, we can limit the direction of incident gamma-rays as an arc, not a cone. Electron tracking method is commonly used for gas detectors [22] and also for solid state detectors in higher energy band [5]. However, our low-noise readout enables us to utilize this method in lower energy band.

In order to demonstrate the full Compton reconstruction with our prototype Si/CdTe Compton telescope, we irradiated it with 662 keV gamma-rays from  $^{137}\text{Cs}$  and analyzed the obtained data. First, we selected “three-hit events”, two hits in successive layers of the DSSDs and one hit in a CdTe pixel detector, from all the data. Then, we solved the Compton kinematics under the hypotheses that

- incident gamma-rays are scattered in the upper layer of the DSSDs,
- recoil electrons stop in the lower layer of the DSSDs,
- scattered gamma-rays are absorbed in the CdTe detector.

In the calculation of Compton kinematics, the angles between the direction of recoil electrons and that of scattered gamma-rays ( $\alpha$ ; see Fig. 6) are able to be determined in two independent ways: from hit positions ( $\alpha_{\text{geom}}$ ) and from deposited energy ( $\alpha_{\text{kin}}$ ), as

$$\alpha_{\text{geom}} = \arccos(\vec{e} \cdot \vec{g}) \quad (3)$$

$$\alpha_{\text{kin}} = \arccos \left[ \left( 1 - \frac{m_e c^2}{E_2} \right) \sqrt{\frac{E_1}{E_1 + 2m_e c^2}} \right], \quad (4)$$

where  $\vec{e}$  and  $\vec{g}$  are the unit vectors with the direction of the recoiled electrons and that of scattered gamma-rays, respectively. By selecting the events which satisfy

$$\alpha_{\text{geom}} \simeq \alpha_{\text{kin}}, \quad (5)$$

background events can be rejected [23]. We calculated this angle from these two methods, and selected events which showed consistent results, i.e. the difference between the angles are less than  $40^\circ$ . For the selected events, we drew arcs in the sky and obtained images.

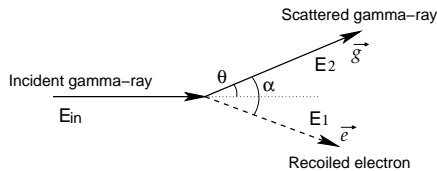


Fig. 6. Definition of the angle  $\alpha$ , the vector  $\vec{e}$ , and  $\vec{g}$

The total number of “three-hit events” (two hits in successive layers of the DSSDs and one hit in a CdTe detector) is measured to be 5 % of that of “two-hit events” (one hit in a DSSD and one hit in a CdTe). After the kinematical selection of Eq. 5, 95 % of “three-hit events” are rejected (see Fig. 7). The rejected events include those in which the scattered gamma-rays are not fully absorbed in CdTe. Also there are events in which the recoil electrons are significantly deflected due to multiple scattering in Si. The events after the selection contain very small portion of background events. Such events are misidentified much more if we do not use the information of the electron track. Since the effect of the multiple scattering becomes smaller for electrons with higher energy, efficiency of this method is expected to be improved for higher energy gamma-rays above MeV. Due to the limited dynamic range of VA32TA chips used in this experiment, demonstration with MeV gamma-rays are not performed here.

Fig. 8 shows the reconstructed image of 662 keV gamma-rays from  $^{137}\text{Cs}$  with the “three-hit events” which satisfy the selection. In drawing the image, the width and the length of each arc are evaluated from the energy resolution and position resolution of the component detectors. We also reconstructed a spectrum by selecting the events, the calculated incident directions of which is within  $30^\circ$  from the source position in the image. The spectrum is shown with solid line in Fig. 7. The 662 keV peak is clearly identified.

## 4 Development for the Next Prototype

### 4.1 4 cm × 4 cm DSSD

With the prototype Compton telescope, we have succeeded in demonstrating the basic performance of a Si/CdTe Compton telescope. As the next step, we are now developing a new prototype with larger area ( $\sim 5 \text{ cm} \times 5 \text{ cm}$ ) and larger volume ( $\sim 20$  layers), in order to improve detection efficiency. For this purpose, we have developed larger DSSDs with dimensions of  $4 \text{ cm} \times 4 \text{ cm}$ . Fig. 9 is the photo of the DSSD module. The strip length is 3.84 cm, and 96 strips are implanted on each side. The thickness, strip pitch, and the gap between the strips are the same as the 2.56 cm wide DSSDs utilized in the



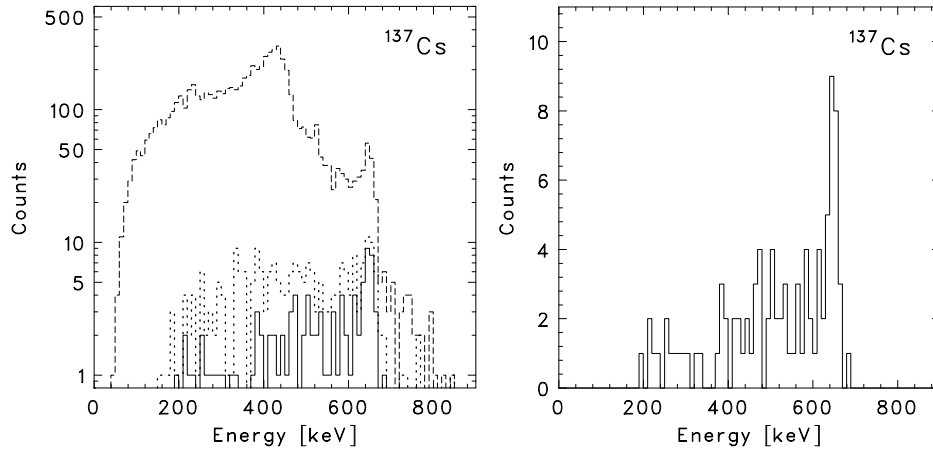


Fig. 7. Reconstructed spectra of  $^{137}\text{Cs}$  with full Compton reconstruction. Left: all the “three-hit events” (the dashed line), the events after kinematical selection (the dotted line), and the events with incoming direction within  $30^\circ$  from the source position (the solid line) are presented. Right: the same as the solid line in the left panel, with linear scale.

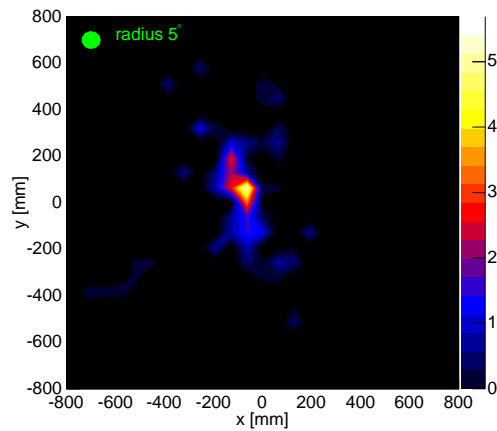


Fig. 8. An image of  $^{137}\text{Cs}$  obtained from the Compton reconstruction with electron tracking.

prototype described above. Measured leakage current per strip is 1 nA at  $23^\circ\text{C}$  when a bias voltage of 100 V is applied. Both the body capacitance and the inter-strip capacitance of a p-strip are 5 pF when fully depleted.

We read out signals from all 192 channels with six VA32TA chips. The p-strips are connected directly to the input pads of the ASICs, while the n-strips are connected via coupling capacitors. Fig. 10 (left) shows a shadow image obtained with the DSSD. The shadow mask is a bookmark made of brass with a thickness of 0.8 mm. The image is created by irradiating the DSSD with 22 keV X-rays from  $^{109}\text{Cd}$ . Several strips with no count were noisy and the triggers were disabled.

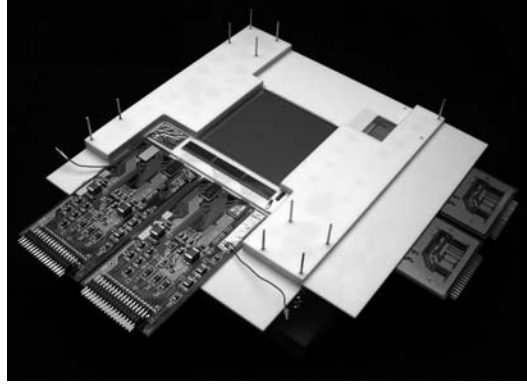


Fig. 9. Photo of the 4 cm  $\times$  4 cm DSSD.

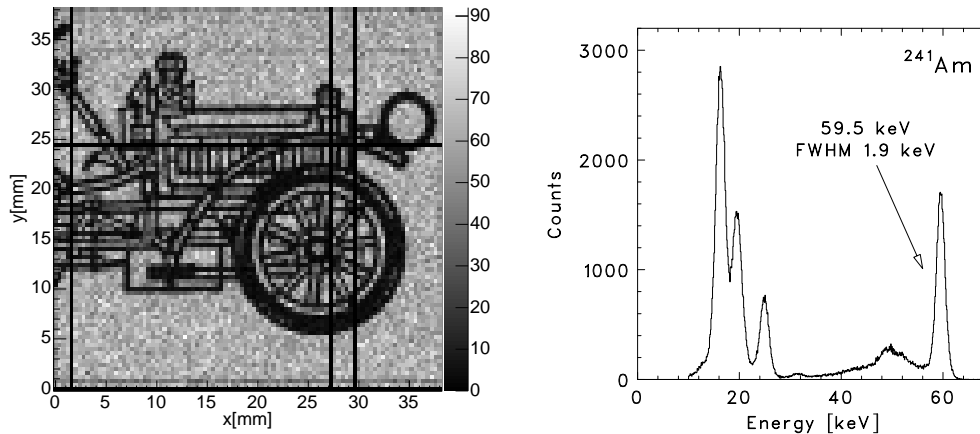


Fig. 10. A shadow image using 22 keV X-rays obtained with the 4 cm  $\times$  4 cm DSSD (left) and a spectrum of  $^{241}\text{Am}$  obtained with the DSSD.

A spectrum of  $^{241}\text{Am}$  obtained with the DSSD is shown in Fig. 10 (right). In the measurement, the DSSD is operated at  $-10\text{ }^\circ\text{C}$  with a bias of 100 V. The energy resolution is 1.9 keV (FWHM) for 60 keV gamma-rays. This value is a little larger than the expected value which is calculated from the leakage current and capacitance of the DSSD. The second device is under construction for further analyses.

#### 4.2 VA64TA ASIC

Larger detector requires larger number of channels to be read out. Because of the thermal designing, lower power per channel is also critical. As the next step to increase the number, we have developed a new analog ASIC, VA64TA, with Ideas.

VA64TA is a 64-channel low-noise analog ASIC, fabricated in the AMS  $0.35\text{ }\mu\text{m}$

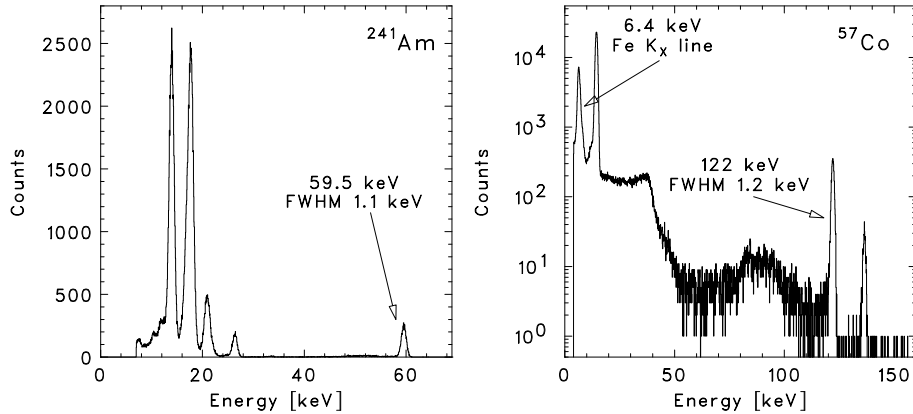


Fig. 11. Spectra of gamma-rays from  $^{241}\text{Am}$  (left) and  $^{57}\text{Co}$  (right) obtained with a silicon strip detector connected to VA64TAs.

technology. The architecture of the chip is based on VA32TA, and each channel circuit includes charge sensitive preamplifier - slow CR-RC shaper - sample/hold - analog multiplexier chain (VA section) and fast shaper - discriminator chain (TA section). The shaping time of the slow shaper is variable from  $3\ \mu\text{s}$  to  $5\ \mu\text{s}$ , and that of the fast shaper is  $600\ \text{ns}$ . The expected noise performance is  $(40 + 12 \times C_d) / \sqrt{\tau}\ \text{e}^-$  (rms) in ENC, where  $C_d$  is the load capacitance in pF and  $\tau$  is the peaking time in  $\mu\text{s}$ . The measured power consumption is  $0.4\ \text{mW}$  per channel, about an order of magnitude lower than the VA32TA chips previously used.

We have tested the VA64TA chips, to which we directly connected a single-sided silicon strip detector (SSSD). The SSSD is fabricated in the same process as the DSSD utilized in our prototype Compton telescope. The strip length is  $1.28\ \text{cm}$ , and the strip pitch is  $400\ \mu\text{m}$  with the gap of  $100\ \mu\text{m}$ . The thickness of the detector is  $300\ \mu\text{m}$ .

The detector module was operated at  $-10\ ^\circ\text{C}$ , and the peaking time of the shaper was set to  $3\ \mu\text{s}$ . The obtained spectra in Fig. 11 shows good noise performance of VA64TA chips. The energy resolution is  $1.1\ \text{keV}$  and  $1.2\ \text{keV}$  (FWHM) at  $59.5\ \text{keV}$  and  $122\ \text{keV}$ , respectively. The energy threshold is as low as  $\sim 4\ \text{keV}$ , and the  $6.4\ \text{keV}$  line is seen in the  $^{57}\text{Co}$  spectrum. The energy resolution obtained with VA64TAs is the same value as that of VA32TAs when connected to the same SSSD.

## 5 Conclusion

We developed a prototype Si/CdTe semiconductor telescope which consists of six-layer DSSDs and three CdTe pixel detectors. With the prototype, we have succeeded in Compton reconstruction and have achieved an angular resolution

of  $3.9^\circ$  (FWHM) for 511 keV gamma-rays and an energy resolution of 14 keV at the same energy. We also succeeded in Compton reconstruction with recoil electron tracking for 662 keV gamma-rays. This approach is thought to be more effective for MeV region.

For the next prototype, we have developed  $4\text{ cm} \times 4\text{ cm}$  DSSDs and a new low-noise and low-power analog ASIC, VA64TA. With the larger DSSD, we have obtained an energy resolution of 1.9 keV for 60 keV gamma-rays. VA64TA chips have operated properly, and their performance is in the same level as VA32TA. With these new technologies, we are now developing a new prototype Compton telescope with 20 layers or more.

## References

- [1] T. Kamae, R. Enomoto, N. Hanada, Nucl. Instr. and Meth. A 260 (1987) 254.
- [2] Y. F. Du, Z. He, G. F. Knoll, D. K. Wehe, W. Li, Nucl. Instr. and Meth. A 457 (2001) 203.
- [3] J. D. Kurfess, W. N. Johnson, R. A. Kroeger, B. F. Philia, E. A. Wulf, Nucl. Instr. and Meth. A 505 (2003) 256.
- [4] T. J. O'Neill, D. Bhattacharya, M. Polsen, A. D. Zych, J. Samimi, A. Akyuz, IEEE Trans. Nucl. Sci. NS-50 (2003) 251.
- [5] G. Kanbach, R. Andritschke, F. Schopper, V. Schönfelder, A. Zoglauer, P. F. Bloser, S. D. Hunter, J. A. Ryan, M. McConnell, V. Reglero, G. DiCocco, J. Knödlseher, New Astron. Rev. 48 (2004) 275.
- [6] T. Takahashi, K. Nakazawa, T. Kamae, H. Tajima, Y. Fukazawa, M. Nomachi, M. Kokubun, Proc. SPIE 4851 (2002) 1228.
- [7] T. Takahashi, K. Makishima, Y. Fukazawa, M. Kokubun, K. Nakazawa, M. Nomachi, H. Tajima, M. Tashiro, Y. Terada, New Astron. Rev. 48 (2004) 269
- [8] T. Mitani, T. Tanaka, K. Nakazawa, T. Takahashi, T. Takashima, H. Tajima, H. Nakamura, M. Nomachi, T. Nakamoto, Y. Fukazawa, IEEE Trans. Nucl. Sci. NS-51 (2004) 2432.
- [9] T. Tanaka, T. Mitani, K. Nakazawa, K. Oonuki, G. Sato, T. Takahashi, K. Tamura, S. Watanabe, H. Tajima, H. Nakamura, M. Nomachi, T. Nakamoto, Y. Fukazawa, Proc. SPIE 5501 (2004) 229.
- [10] S. Watanabe, T. Tanaka, K. Nakazawa, T. Mitani, K. Oonuki, T. Takahashi, T. Takashima, H. Tajima, Y. Fukazawa, M. Nomachi, S. Kubo, M. Onishi, Y. Kuroda, IEEE Trans. Nucl. Sci. (2005) in press.
- [11] A. Zoglauer, G. Kanbch, Proc. SPIE 4851 (2003) 1302

- [12] K. Yamashita, P. J. Serlemitsos, J. Tueller et al., *Applied Optics* 37 (1998) 8067
- [13] T. Takahashi, A. Awaki, T. Dotani, Y. Fukazawa, K. Hayashida, T. Kamae, J. Kataoka, N. Kawai, S. Kitamoto, T. Kohmura, M. Kokubun, K. Koyama, K. Makishima, H. Matsumoto, E. Miyata, T. Murakami, K. Nakazawa, M. Nomachi, M. Ozaki, H. Tajima, M. Tashiro, T. Tamagawa, Y. Terada, H. Tsunemi, T. Tsuru, K. Yamaoka, D. Yonetoku, A. Yoshida, *Proc. SPIE* 5488 (2004) 549.
- [14] T. Takahashi, K. Nakazawa, S. Watanabe, G. Sato, T. Mitani, T. Tanaka, K. Oonuki, K. Tamura, H. Tajima, T. Kamae, G. Madejski, M. Nomachi, Y. Fukazawa, K. Makishima, M. Kokubun, Y. Terada, J. Kataoka, M. Tashiro, *Nucl. Instr. and Meth. A* 541 (2005) 332.
- [15] H. Tajima, T. Kamae, G. Madejski, T. Mitani, K. Nakazawa, T. Tanaka, T. Takahashi, S. Watanabe, Y. Fukazawa, T. Ikagawa, J. Kataoka, M. Kokubun, K. Makishima, Y. Terada, M. Nomachi, M. Tashiro, *IEEE Trans. Nucl. Sci.* (2005) in press.
- [16] H. Tajima, T. Kamae, S. Uno, T. Nakamoto, Y. Fukazawa, T. Mitani, T. Takahashi, K. Nakazawa, Y. Okada, M. Nomachi, *Proc. SPIE* 4851 (2002) 875.
- [17] H. Tajima, T. Nakamoto, T. Tanaka, S. Uno, T. Mitani, E. do Couto e Silva, Y. Fukazawa, T. Kamae, G. Madejski, D. Marlow, K. Nakazawa, M. Nomachi, Y. Oakada, T. Takahashi, *IEEE Trans. Nucl. Sci.* NS-51 (2004) 842.
- [18] Ideas ASA, <http://www.ideas.no/>
- [19] T. Takahashi, B. Paul, K. Hirose, C. Matsumoto, R. Ohno, T. Ozaki, K. Mori, Y. Tomita, *Nucl. Instr. and Meth. A* 436 (2000) 111.
- [20] Y. Fukazawa, T. Nakamoto, N. Sawamoto, S. Uno, T. Ohsugi, H. Tajima, T. Takahashi, T. Mitani, T. Tanaka, K. Nakazawa, *Proc. SPIE* 5501 (2004) 197.
- [21] T. Mitani, H. Nakamura, S. Uno, T. Takahashi, K. Nakazawa, S. Watanabe, H. Tajima, M. Nomachi, Y. Fukazawa, S. Kubo, Y. Kuroda, M. Onishi, R. Ohno, *IEEE Trans. Nucl. Sci.* NS-50 (2003) 1048.
- [22] T. Tanimori, H. Kubo, K. Miuchi, T. Nagayoshi, R. Orito, A. Takada, A. Takeda, M. Ueno, *New Astron. Rev.* 48 (2004) 263.
- [23] R. Orito, H. Kubo, K. Miuchi, T. Nagayoshi, A. Takada, A. Takeda, T. Tanimori, M. Ueno, *Nucl. Instr. and Meth. A* 525 (2004) 107.